frontier
in Human Neuroscience

Network Construction

Figure 1

Network Node Definition

White Matter Tractography

Network Edge Definition

Identification of Pivotal Edges

B_i^{edge}

B_i^{edge}

$$B_i^{edge} = \sum_{j \neq k} \frac{\sigma_{j,\,k(i)}}{\sigma_{j,\,k}}$$

j k
i
$\sigma_{j,k}$
j k $\sigma_{j,k\,i}$
j k i

$$b_i^{edge} = \frac{B_i^{edge} - \mathrm{mean}\left(B_i^{edge}\right)}{\mathrm{std}\left(B_i^{edge}\right)}$$

mean B_i^{edge} std B_i^{edge}

b_i^{edge} >
>

P x $\sim \alpha x^{\beta}$ P x $\sim \alpha$ βx
P x $\sim \alpha x^{\beta}$ x γ

<
°

The Wiring Substrates of the Pivotal Edges

Network Analysis

$$FA = \sqrt{-\frac{\sqrt{\left(\lambda - \tilde{\lambda}\right) - \left(\lambda - \tilde{\lambda}\right) - \left(\lambda - \tilde{\lambda}\right)}}{\sqrt{\lambda + \lambda + \lambda}}}$$

$\tilde{\lambda} = (\lambda + \lambda + \lambda)/$

$$MD = \lambda + \lambda + \lambda$$

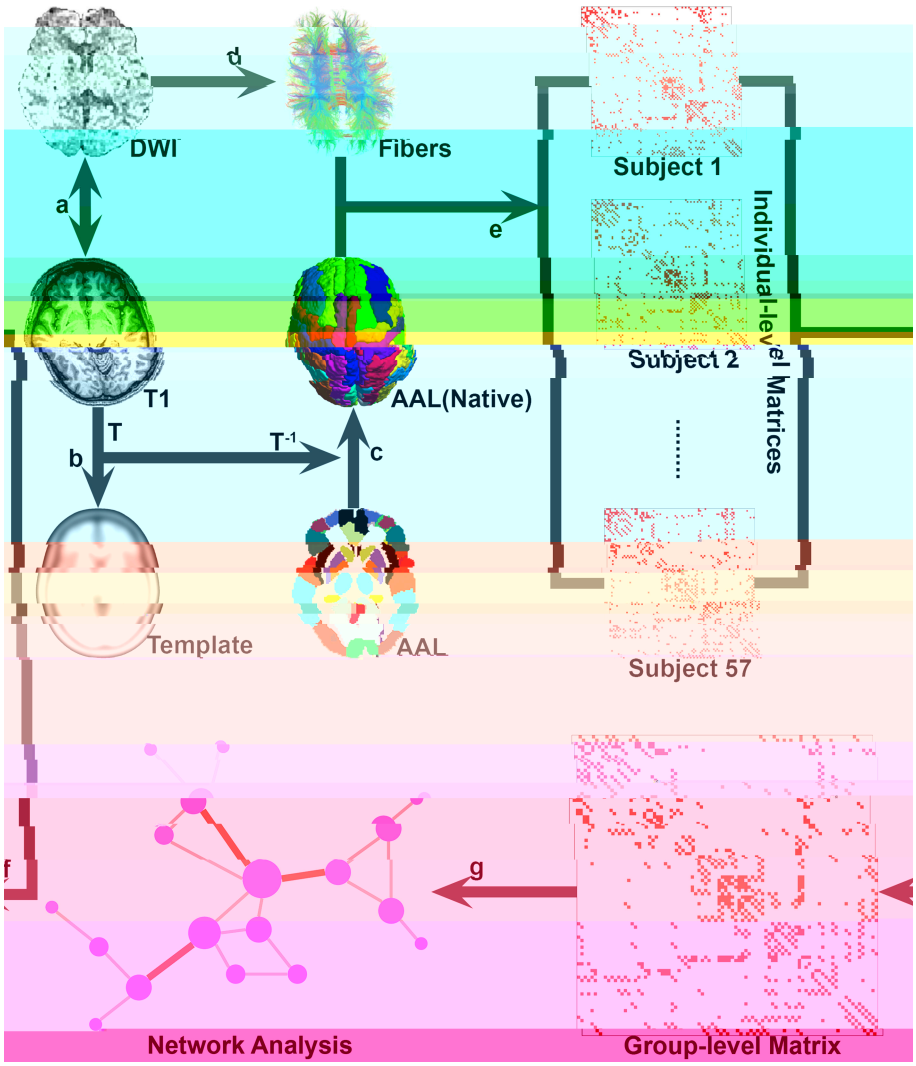

FIGURE 1 | A flowchart for the construction of the whole-brain WM network. (A) The T1-weighted image was firstly rigidly coregistered to the averaged b0 image in native diffusion space; **(B)** The transformed T1 image was then nonlinearly transformed to the ICBM152 T1 template in the MNI space, and the transformation matrix T was estimated; **(C)** the inversed transformation T-1 was used to warp the AAL atlas from the MNI space to the native diffusion space, obtaining the parcellation for each individual; **(D)** the whole-brain WM tracts were reconstructed by using deterministic tractography; **(E)** the WM fibers connecting each pair of regions were determined for each subject, thus the individual WM networks were constructed; **(F)** the group-level connectivity matrix was computed by selecting all connections that were present in at least 50% of the group of individuals; and **(G)** both the individual and group-level networks were further analyzed by using graph theoretical methods.

$$\mathbf{AD} = \lambda$$

$$\mathbf{RD} = \lambda + \lambda$$

Contributions to the Nodal Centralities

K_i

$$K_i = \sum_{j \in N} a_{ij}$$

$a_{ij} =$ i j

$$E_i = \frac{\sum_{j \in N, j \neq i} L_{ij}^{-}}{N -}$$

L_{ij}^{-} i j B_i^{node}

$$B_i^{node} = \sum_{j \neq k \neq i} \rho_{j,k(i)}$$

$\rho_{j,k\ i}$ j k i

Contributions of the Pivotal Edges to the Rich-Club Structure

chance

$\Phi\ k$

$$\Phi(k) = \frac{E_{>k}}{N_{>k}(N_{>k} -)}$$

k $E_{>k}$ $N_{>k}$ $\Phi\ k$ $\Phi_{norm\ k}$ $\Phi\ k$

$$\Phi_{norm}(k) = \frac{\Phi(k)}{\Phi_{random}(k)}$$

$\Phi_{random}\ k$ $\Phi_{norm}\ k\ >$ k k $\Phi_{norm}\ k$ $k\ =$ $k\ >$

Communication Length and Path Motifs

$n \times (n -) / \quad n = 90$

Validation Analysis

Vulnerability and Network Robustness

Edge Betweenness and Pivotal Edges in the WM Networks

Edge Betweenness Distribution

TABLE 1 | The pivotal edges of the human brain WM network and their properties.

No.	Region A	Region B	Normalized EBC	Fiber Length (mm)	Class	Lobes	WM tracts	Connection category	Vulnerability (%)
1	PoCG.R	PCu.L	5.33	114.84	InterHemi	LP-RP	CC	Feeder	0.333
2	PCu.L	STG.L	5.26	87.92	InterLobe	LP-LT	Short tract	Feeder	0.242
3	PCu.L	PUT.L	4.93	88.92	InterLobe	LP-LS	Projection tract	Rich-club	0.212
4	ORBsup.L	ORBsup.R	4.79	86.84	InterHemi	LF-RF	CC	Rich-club	0.287
5	PCu.R	STG.R	3.75	87.45	InterLobe	RP-RT	Short tract	Feeder	0.248
6	PCu.R	PUT.R	3.73	81.81	InterLobe	RP-RS	Projection tract	Rich-club	0.250
7	HIP.L	HIP.R	3.53	92.38	InterHemi	LT-RT	CC	Local	0.395
8	SFGdor.R	IFGtriang.L	3.36	98.42	InterHemi	LF-RF	CC	Feeder	0.220
9	HES.L	STG.L	3.29	18.61	IntraLobe	LT-LT	Short tract	Local	1.505
10	HES.R	STG.R	3.29	14.82	IntraLobe	RT-RT	Short tract	Local	1.456
11	SPG.L	SPG.R	3.17	114.43	InterHemi	LP-RP	CC	Local	0.153
12	SPG.R	PCu.L	2.92	111.02	InterHemi	LP-RP	CC	Feeder	0.102
13	ORBsup.R	ITG.R	2.72	76.77	InterLobe	RF-RT	UF	Feeder	0.240
14	SOG.R	MOG.L	2.62	137.84	InterHemi	LR-RO	CC	Rich-club	0.162
15	CAL.R	PCu.L	2.53	68.02	InterHemi	LP-RO	CC	Rich-club	0.156
16	SPG.L	PCu.R	2.42	105.99	InterHemi	LP-RP	CC	Feeder	0.139
17	PCu.L	MTG.L	2.35	90.80	InterLobe	LP-LT	Cingulum	Feeder	0.111
18	PHG.L	PCu.L	2.25	39.17	InterLobe	LP-LT	Cingulum	Feeder	0.199
19	SFGdor.R	ORBsup.R	2.14	13.82	IntraLobe	RF-RF	Short tract	Rich-club	0.149
20	ACG.L	PCu.L	2.03	75.95	InterLobe	LF-LP	Cingulum	Feeder	0.218
21	MOG.L	PUT.L	1.84	89.45	IntraLobe	LO-LS	IFO	Rich-club	0.107
22	SFGdor.L	SFGdor.R	1.78	89.09	InterHemi	LF-RF	CC	Feeder	0.065
23	ORBsup.R	TPOmid.R	1.78	70.34	InterLobe	RF-RT	UF	Feeder	0.111
24	PCu.L	PCL.L	1.70	13.62	IntraLobe	LP-LP	Short tract	Feeder	0.172
25	HIP.R	THA.R	1.70	40.31	InterLobe	RT-RS	Undefined	Local	0.196
26	CAL.L	PCu.R	1.67	63.70	InterHemi	RP-LO	CC	Rich-club	0.143
27	PreCG.R	PCL.L	1.65	125.33	InterHemi	RF-LP	CC	Local	0.142
28	PCu.L	THA.L	1.63	70.58	InterLobe	LP-LS	Projection tract	Feeder	0.102
29	DCG.L	PCu.L	1.60	33.52	InterLobe	LF-LP	Cingulum	Feeder	0.176
30	ORBsup.R	PUT.R	1.59	38.59	InterLobe	RF-RS	Projection tract	Rich-club	0.097
31	PHG.R	PCu.R	1.57	40.99	InterLobe	RP-RT	Cingulum	Feeder	0.121
32	DCG.R	PCu.R	1.55	32.99	InterLobe	RF-RP	Cingulum	Feeder	0.190
33	ORBsup.L	ITG.L	1.54	70.46	InterLobe	LF-LT	UF	Feeder	0.149
34	PCu.L	PCu.R	1.53	96.65	InterHemi	LP-RP	CC	Rich-club	0.056
35	ACG.R	PCu.R	1.48	84.79	InterLobe	RF-RP	Cingulum	Feeder	0.181
36	CAU.L	PUT.L	1.42	11.21	IntraLobe	LS-LS	Undefined	Feeder	0.116
37	SOG.R	PCu.L	1.40	93.38	InterHemi	LP-RO	CC	Rich-club	0.079
38	ORBinf.L	MOG.L	1.38	137.25	InterLobe	LF-RO	IFO	Feeder	0.158
39	PUT.R	PAL.R	1.34	12.63	IntraLobe	RS-RS	Undefined	Feeder	0.133
40	PCu.L	PCL.R	1.30	111.80	InterHemi	LP-RP	CC	Feeder	0.218
41	SFGdor.R	PUT.R	1.28	48.90	InterLobe	RF-RS	Projection tract	Rich-club	0.074
42	PCG.R	PCu.L	1.20	33.89	InterHemi	LP-RP	CC	Feeder	0.162
43	ORBinf.R	CAL.R	1.17	144.23	InterLobe	RF-RO	IFO	Feeder	0.123
44	ORBsup.L	INS.L	1.12	18.42	InterLobe	LF-LS	UF	Feeder	0.134
45	PreCG.R	MTG.R	1.11	95.09	InterLobe	RF-RT	Short tract	Local	0.128
46	CAU.L	THA.L	1.07	25.22	IntraLobe	LS-LS	Undefined	Local	0.116

(Continued)

TABLE 1 | Continued

No.	Region A	Region B	Normalized EBC	Fiber Length (mm)	Class	Lobes	WM tracts	Connection category	Vulnerability (%)
47	PUT.L	PAL.L	1.06	12.18	IntraLobe	LS-LS	Undefined	Feeder	0.102
48	CAU.R	PUT.R	1.04	11.82	IntraLobe	RS-RS	Undefined	Feeder	0.097

Fiber tracts were determined by examining the tractography result of each individual with prior anatomical knowledge. No., number; EBC, edge betweenness centrality; PoCG, postcentral gyrus; R, right; PCu, precuneus; L, left; ORBsup, superior frontal gyrus, orbital part; HIP, hippocampus; SFGdor, superior frontal gyrus, dorsolateral; HES, Heschl gyrus; SPG, superior parietal gyrus; SOG, superior occipital gyrus; CAL, calcarine fissure and surrounding cortex; PHG, parahippocampal gyrus; ACG, anterior cingulate and paracingulate gyri; PreCG, precentral gyrus; DCG, median cingulate and paracingulate gyri; CAU, caudate nucleus; ORBinf, inferior frontal gyrus, orbital part; PCG, posterior cingulate gyrus; PUT, putamen; STG, superior temporal gyrus; IFGtriang, inferior frontal gyrus, triangular part; ITG, inferior temporal gyrus; MOG, middle occipital gyrus; MTG, middle temporal gyrus; TPOmid, temporal pole: middle temporal gyrus; PCL, paracentral lobule; THA, thalamus; INS, insula; InterHemi, inter-hemispheric connection; InterLobe; intra-hemispheric inter-lobe connection; IntraLobe, within lobe connections; LP, left parietal lobe; RP, right parietal lobe; LT, left temporal lobe; LS, left subcortical; LF, left frontal lobe; RF, right frontal lobe; RT, right temporal lobe; RS, right subcortical; RO, right occipital; LO, left occipital; CC, corpus callosum; UF, uncinate fasciculus; IFO, inferior frontooccipital fasciculus.

The Wiring Substrates of the Pivotal WM Edges

$p <$ **Figure 2D**

$p =$

$p <$ **Figure 2E**

$\rho =$ $p <$

$p <$

Figure 2E

Figure 2F

Contributions of the Pivotal Edges to the Network Hubs/Rich-Club Structure

Contribution to the Nodal Properties

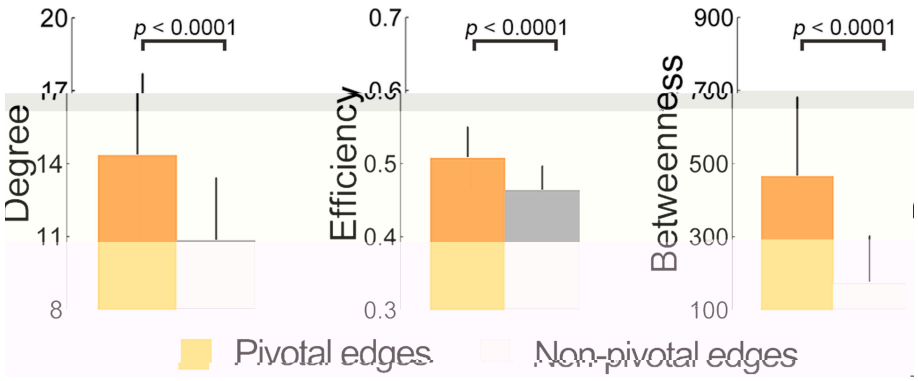

FIGURE 3 | Contribution of the pivotal edges toward the centrality of the nodes they linked. The pivotal edges had significantly greater contributions to all three nodal properties (nodal degree, efficiency, and betweenness) than the non-pivotal ones. The contribution toward nodal centralities of an edge was estimated by averaging nodal properties of its two linking nodes.

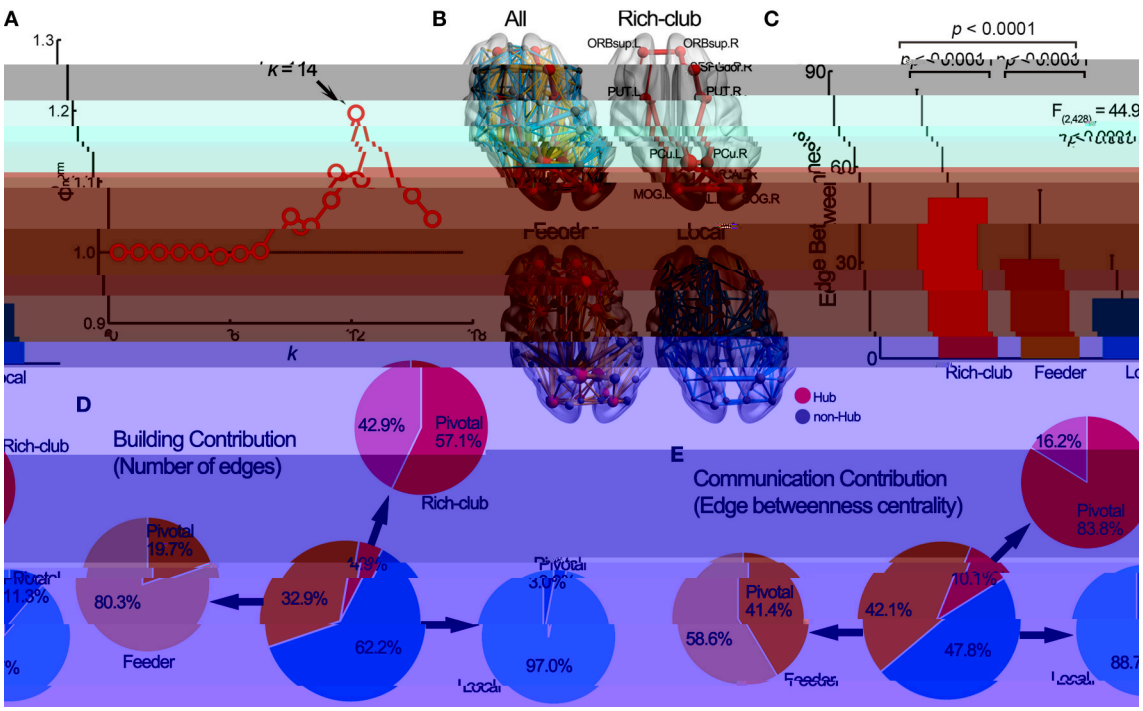

FIGURE 4 | Pivotal edges and the rich-club structure. (A) The normalized rich-club coefficient $\Phi_{norm}(k)$ of the group-level WM network was above 1 for a range of k from 9 to 16. The peak at $k = 14$ was selected as the hub threshold for further analysis. **(B)** The network hubs were mainly located in the medial line of the brain and the connections of the brain network can be further classified into three categories: rich-club (red), feeder (yellow) and local (blue) connections. **(C)** The edge betweenness centrality values were significantly different among rich-club, feeder, and local connections. **(D)** The pivotal edges had significantly different building contribution (indicated by the proportion of number) to three categories of connections. **(E)** The communication contribution (indicated by the proportion of edge betweenness centrality), of the pivotal edges was also significantly different among three categories of connections. The center pie illustrates the building/communication percentage of the three types of connections, and the surrounding pies show the building/communication percentage in each category of the connections. SFGdor, superior frontal gyrus, dorsolateral; CAL, Calcarine fissure and surrounding cortex; L, left; R, right. For other abbreviations, see **Figure 2**.

Communication Length and Path Motifs

Communication Length of Pivotal Edges

$p <$ **Figure 6A**

Table 1

Path Motifs of the WM Network

Figures 6B,C

Figure 5A

Validation Results

$>$ **Figure 5B**

$Z =$

Path Motifs across Different Brain Systems

DISCUSSION

Figure 5C

Spatial Distribution of Pivotal WM Connections

Lesion Simulations

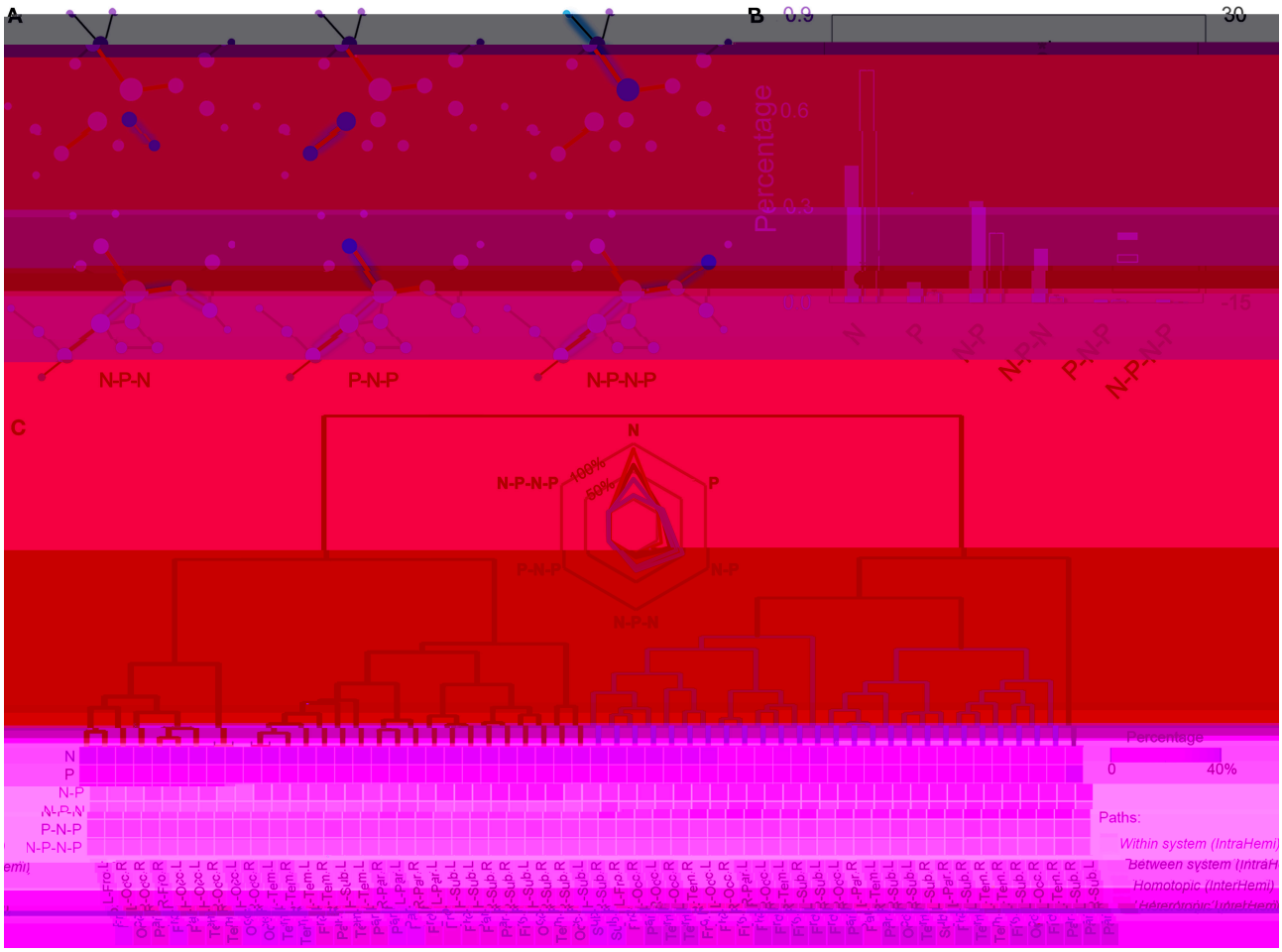

FIGURE 5 | Path motifs of the whole-brain WM network and of different brain systems. (A) Examples of the six types of path motifs in the whole-brain WM network. Path motifs were defined as the ordered sequence of the pivotal or the non-pivotal edges on the routes of each shortest path. N, non-pivotal edge; P, pivotal edge. **(B)** The frequency percentage and normalized distribution of path motifs derived by comparing the actual frequency of each path motif to that of 1000 equivalent random networks. The "non-pivotal to pivotal to non-pivotal" (N-P-N) path motif was the most frequent path motif in the brain network ($Z = 23.1$). **(C)** The bottom matrix shows the proportions of path motifs between each pair of the brain systems. The following hierarchical clustering analysis revealed four path-motif distribution patterns, of which the path motif "N" decreased gradually while the "P" related path motifs constantly accumulated. Notably, most within-system and intra hemispheric paths communicated with the style "N," while the inter-hemispheric paths, especially paths between heterotopic systems, utilized the pivotal edges more often. Fro, frontal; L, left; Occ, occipital; R, right; Par, parietal; Tem, temporal; Sub, subcortical; IntraHemi, intra hemispheric; InterHemi, inter hemispheric.

The WM Microstructural Organization and Wiring Cost of the Pivotal WM Connections

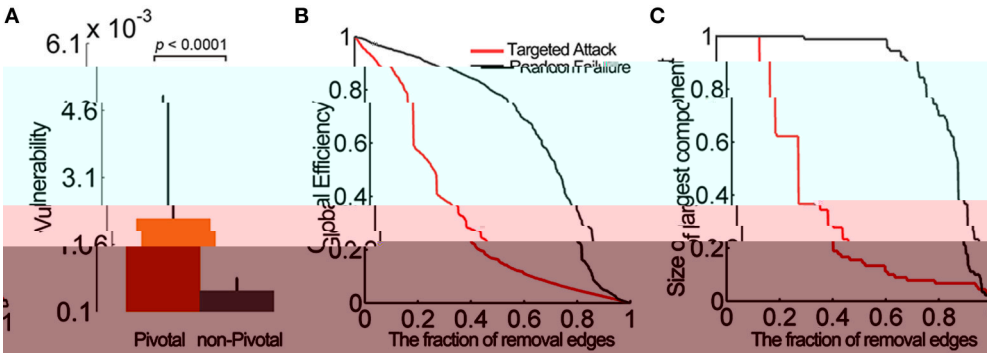

FIGURE 6 | Vulnerability of the pivotal edges and lesion simulation. (A) The pivotal edges showed significant greater vulnerability than the non-pivotal ones. The error bars represent the standard deviation. **(B)** The global efficiency and **(C)** the size of largest connected component slowly declined in the random failure. When facing the targeted attacks, these network properties decreased rapidly (over 40%) after the top 20% edges were removed.

Contributions of the Pivotal Edges toward the Network Hubs/Rich-Club Architectures

Utilization of the Pivotal WM Connections in Communication Strategy

Magn. Reson. Med.

NMR Biomed.

NMR Biomed.

Nature Physics

J. Neurosci.

Nat. Rev. Neurosci.

Neuron

in vivo Magn. Reson. Med.

Cereb. Cortex

Proc. Natl. Acad. Sci. U.S.A.

Brain

J. Neurosci.

Philos. Trans. R. Soc. Lond. B. Biol. Sci.

Neuroimage

J. Neurosci.

Sociometry

Brain

Proc. Natl. Acad. Sci. U.S.A.

functionnal connectivi (2004) Mappin t. Esoceu, Sr(t)104(d)-6(d)-6(f-299662

Neuroimage

Front. Hum. Neurosci.

PLoS ONE

PLoS Comput. Biol.

Neuroimage

Nature

PLoS ONE

Proc. Natl. Acad. Sci. U.S.A.

Proc. Natl. Acad. Sci. U.S.A.

Proc. Natl. Acad. Sci. U.S.A.

Neuroimage

Conflict of Interest Statement

Neuroimage

Proc. Natl. Acad. Sci. U.S.A.

Proc. Natl. Acad. Sci. U.S.A.

J. Neurosci.

Trends Cogn. Sci.

Proc. Natl. Acad. Sci. U.S.A.